Nanoplastics promote microcystin synthesis and release from cyanobacterial *Microcystis aeruginosa*

Li-Juan Feng[a], Jia-Qi Liu[a], Lin-Lin Zhou[a], Fan-Ping Zhu[a], Xiao-Dong Sun[a], Xiao-Yu Liu[a], Shu-Guang Wang[a], Tamara Susan Galloway[b*], Xian-Zheng Yuan[a*]

a Shandong Key Laboratory of Water Pollution Control and Resource Reuse, School of Environmental Science and Engineering, Shandong University, Qingdao, Shandong 266237, P. R. China

b College of Life and Environmental Sciences, University of Exeter, Exeter EX4 4QD, Devon, United Kingdom

Corresponding authors:

Xian-Zheng Yuan

School of Environmental Science and Engineering, Shandong University

72 Rd. Binhai, Qingdao, Shandong 266237, P. R. China

E-mail: xzyuan@sdu.edu.cn

Tamara Susan Galloway

College of Life and Environmental Sciences, University of Exeter

Exeter EX4 4QD, Devon, United Kingdom

Email: t.s.galloway@exeter.ac.uk

Although the fate of nanoplastics (< 100 nm in size) in freshwater systems is increasingly well studied, much less is known about its potential threats to cyanobacterial blooms, as the ultimate phenomenon of eutrophication occurring world-wide. A handful of studies has evaluated the consequences of nanoplastics increasing the membrane permeability of microbes, but there is no direct evidence for interactions between nanoplastics and microcystin; intracellular hepato-toxins produced by some genera of cyanobacteria. Here we show that amino-modified polystyrene nanoplastics (PS-NH_2) promote microcystin synthesis and release from *Microcystis aeruginosa*, a dominant species causing cyanobacterial blooms. We demonstrate that PS-NH_2 inhibits photosystem II efficiency, reduces organic substance synthesis, and induces oxidative stress, enhancing the synthesis of microcystin. Furthermore, PS-NH_2 promotes the extracellular release of microcystin from *M. aeruginosa* via transporter protein up-regulation and impaired cell membrane integrity. Our findings propose that the presence of nanoplastics in freshwater ecosystems might enhance the threat of eutrophication to aquatic ecology and human health.

MAIN TEXT

Plastic debris are increasingly considered a global concern due to their negative social and ecological impacts[1,2,3,4]. The discarded plastic can be degraded into microplastics (0.1-5 mm in size), and even nanoplastics (< 100 nm) by abiotic and biotic factors[5]. In addition, nanoplastics are directly derived from personal care and cosmetic products and industrial processes where nanoplastics are used or formed[6,7]. Although the fate and effect of nanoplastics in marine environments are increasingly well studied, much less is known about the ecological effects of nanoplastics in freshwater environments, which have been considered a major source of nanoplastics. In freshwater systems, the cyanobacteria, the extensive occurrence of which is regarded as eutrophication[8], have repeatedly been detected as a main component attached to the plastic surface. Furthermore, a number of cyanobacterial species can produce microcystin, with *Microcystis* as the predominant producer in freshwater systems[9,10]. Microcystin have been associated with liver cancer and fatality, for example with the deaths of 60 patients after renal dialysis with microcystin-contaminated water in Brazil[11,12]. Hence, the interactions between cyanobacteria and nanoplastics in freshwater potentially affects the formation and persistence of cyanobacteria blooms as well as microcystin.

We cultured *M. aeruginosa* in standard blue-green (BG-11) medium containing polystyrene nanoplastics with differential surface charge, to simulate changes caused by weathering of plastics and adsorbing of natural organic matter[13]. We found that the negative-charged sulfonic acid-modified polystyrene nanoplastics (PS-SO_3H) showed no obvious inhibitory effect even when the exposure concentration was 100 μg/mL (Supplementary Figure 1A). Due to electrostatic repulsion, positively charged nanoparticles interact more easily than negatively charged nanoparticles with negative

membrane residuals. Hence, we found positive-charged amino-modified polystyrene nanoplastics (PS-NH_2) had a greater influence on *M. aeruginosa* than negatively charged plastics (Supplementary Figure 1B). During the acute 48-h exposure, growth inhibition of *M. aeruginosa* by low (3.40 μg/mL) and high (6.80 μg/mL) concentrations of PS-NH_2 was 23.57% and 46.10%, respectively, with the normally green *M. aeruginosa* turning yellow (Fig. 1A and B), in parallel with a significant reduction in the chlorophyll-a content (Supplementary Figure 1C). This inhibition was significantly reduced upon long-term exposure (10 days), with *M. aeruginosa* regaining its green coloration (Fig. 1A), indicating that the interaction of nanoplastics and cyanobacteria was dynamic and without persistence within the experimental period. However, the synthesis of microcystin increased significantly both under acute and long-term exposure, compared to the control group (Fig. 1C). And microcystin-leucine-arginine (MC-LR), the most common and harmful microcystin in freshwater environments, also increased significantly (Supplementary Figure 2A). Furthermore, both exposures of PS-NH_2 significantly stimulated the extracellular release of microcystin and MC-LR from *M. aeruginosa* (Fig. 1D; Supplementary Figure 2B).

To identify the molecular mechanisms responsible for the effects described above, the proteomics of *M. aeruginosa* under PS-NH_2-induced stress were performed. The proteomics results revealed that PS-NH_2 had a substantial influence on cyanobacterial growth (Supplementary Figure 3). The proteins that were significantly down-regulated in both low- and high-concentration treatments suggested that PS-NH_2 may inhibit the photosynthetic activity, weaken the photosynthetic electron transport chain, and reduce carbohydrate metabolism (Supplementary Figure 4; Supplementary Table 1). In addition, the acute exposure of low-concentration PS-NH_2 only influenced the

101 light reaction of photosynthesis comparing with both the light and dark reactions of
102 photosynthesis impaired by high-concentration PS-NH_2 treatment (Supplementary
103 Figure. 5A). The main proteins (*psbB*, *psbC*, and *psbD*) involved in photosystem II
104 were all down-regulated (Supplementary Table 1), indicating that the photosynthetic
105 efficiency of photosystem II was significantly inhibited by PS-NH_2. The weakening
106 of the photosynthetic electron transport chain, alleviated gradually by detoxification
107 enzymes for low-concentration exposure and continuing in the later period under
108 high-concentration exposure, lead to the accumulation of surplus electrons and
109 inducedoxidative stress (Supplementary Figure 5B; Supplementary Table 1). The
110 reduction of carbohydrate metabolism was consistent with decreased growth after
111 treatment with PS-NH_2 (Supplementary Figure 5C). Furthermore, the down-
112 regulation of lipopolysaccharide biosynthetic process-related proteins (Supplementary
113 Table 1), involved in synthesizing integral components of the membrane, indicated
114 damage to cell membrane integrity after PS-NH_2 exposure. The exposure to both
115 concentrations of PS-NH_2 led to the up-regulation of proteins involved in the
116 biological transport process (Supplementary Figure 5D; Supplementary Table 1), such
117 as ABC transporters, which are transmembrane complexes that span both the plasma
118 membrane and outer membrane of *M. aeruginosa* and actively export substrates, such
119 as macrolide antibiotics, peptides, virulence factors, and cell envelope precursors[14].
120
121 To verify the above proteomics results, we performed a qRT-PCR assay on *psbD,* a
122 key gene associated with photosynthesis II. Pearson's correlation coefficient between
123 the qRT-PCR data (Fig. 1E) and the proteomics data was 0.80, which indicates the
124 accuracy of the proteomics data. The down-regulation of *psbD* is known to interfere
125 with electron transport, leading to the accumulation of surplus electrons and oxidative

stress[15, 16]. Upon acute exposure of PS-NH_2, we observed a significant increase in the levels of reactive oxygen species (ROS) (Fig. 1G) and superoxide dismutase (SOD) (Supplementary Figure 6A), a part of the cell's antioxidant defense system. The induction of oxidative stress was consistent with the proteomics data. The level of reduced glutathione (GSH) decreased significantly comparing with the untreated control, to eliminate the oxidative stress (Supplementary Figure 6B). For validation of proteomics analysis for cyanobacterial membrane transport, we used green-fluorescent PS-NH_2 to determine whether PS-NH_2 entered and accumulated in *M. aeruginosa*. The behavior of the fluorescently labelled PS-NH_2 was similar to that of PS-NH_2, both in the culture medium and deionized water (Supplementary Figure 7). The fluorescently labelled PS-NH_2 penetrated the cell membrane and accumulated inside the cells (Fig. 1G). The process of the nanoparticles entering the cell appeared to rupture the cell membrane, an effect seen both under acute and long-term exposure to PS-NH_2 (Fig. 1H). Such a membrane rupture could enhance the release of intracellular materials such as microcystin.

Given that the up-regulation for most of the proteins involved in the synthesis of microcystin[17] was not significant (Supplementary Table 2), we built co-expression modules from our proteomic data using weighted gene correlation network analysis (WGCNA). We identified 18 co-expression modules from the data regarding the 2413 proteins from the 18 samples (Fig. 2A and B), and effectively identified three groups of hub proteins (Fig. 2C, D, and E and Supplementary Fig. 8), which were placed in the middle of the protein-protein interaction (PPI) networks (Fig. 2F). The top hub proteins marked with yellow in the brown module, with a negative correlation to the synthesis of intracellular microcystin, are tryptophan synthase C (involved in organic

151 substance metabolic pathways). This indicates that the decrease in synthesis of
152 organic substances stimulates the microcystin synthesis, which protects *M.*
153 *aeruginosa* from oxidative damage.[18] The top hub proteins in the turquoise module
154 (pyrG) and blue module (apcB1 and N44_03141) are positively and negatively
155 correlated with extracellular microcystin, respectively (Supplementary Table 3). The
156 proteins of pyrG and apcB1 are related to the regulation of phospholipid synthesis[19]
157 and thylakoid membrane by module GO enrichment, respectively. Additionally,
158 N44_03141 is an alkaline phosphatase-like protein that is associated with the integral
159 components of the membrane. The up-regulation of pyrG protein may be a defense
160 response against cell membranes damage. Down-regulation of apcB1 and N44_03141
161 was in accordance with the self-protection of thylakoid membrane and damage of cell
162 membrane integrity, respectively. Hence, the increased synthesis of microcystin was
163 a defense response to protect cells from oxidative damage and enhance the fitness of
164 *M. aeruginosa* to the stresses caused by nanoplastics[18,20], which was observed under
165 exposure to antibiotic[21], iron-limiting conditions[18] and herbicide[22]. The damage to
166 membrane integrity and the up-regulation of biological-transport proteins were the
167 main explanation for the stimulated release of microcystin.
168
169 Our study provides a better understanding of the fate, distribution, and molecular
170 basis of nanoplastics in aquatic primary producers, such as cyanobacteria. The extent
171 to which the environment is contaminated with nanoplastics remains to be quantified,
172 given the technical challenge of detecting such small and carbon-based particles in
173 complex natural matrices. However, in the controlled laboratory, 0.3% (w/w) of a
174 polymeric latex film formed nanoparticles with average diameter of 196.52 nm (±
175 89.48) after 200-days exposure into the freshwater environment. Based on the limited

reports on microplastics abundance in Three Gorges Reservoir (1597 to 12,611 items/m^3) and midstream of the Los Angeles River (12,000 items/m)[23], the concentration of nanoplastics in freshwater systems might be in the level of μg/mL, not to mention the meso- or macro-plastics. The exposure to nanoplastics in this concentration in the current study promoted microcystin synthesis and release from *Microcystis aeruginosa*, even without the change of coloration. Cyanobacterial blooms have negative consequences for both human health and aquatic ecology. Cyanobacteria form the base of many food chains; furthermore, the accumulation of nanoplastics in cyanobacteria might have effects on other trophic levels, which could pose a potential risk to food safety.

METHODS

Characterization of Nanoplastics

The PS-NH_2 (50 nm) particles and green fluorescently labelled 50 nm PS-NH_2 particles (excitation wavelength, 475 nm; emission wavelength, 510 nm) were purchased from Bangs Laboratory (USA) and micromod Partikeltechnologie GmbH (Germany), respectively. Sulfonic acid-modified polystyrene nanoplastics (PS-SO_3H) were synthesized in the laboratory through nitrogen-protected emulsion polymerization with styrene as a monomer[24, 25]. Before the experiment, the nanoparticles were transferred to a dialysis bag (1 kDa) for 3 days to remove redundant monomers or initiators[26]. The diameter and morphologies of PS-NH_2 were characterized by a scanning electron microscope (SEM; S-5000, Hitachi, Japan). The size (Z-average) and ζ-potential (mV) were determined using dynamic light scattering (DLS; Zetasizer Nano ZS, Malvern, UK). The structure and composition of nanoplastics (Supplementary Figure 9) were determined via a Fourier transform

infrared (FTIR) spectrometer (Aratar, Thermo NicoLet, USA) at wavenumbers from 4000 to 400 cm^{-1}. Ultraviolet-visible (UV-Vis) spectra (190 - 450 nm) of PS-NH_2 in the aqueous phase were collected using an ultraviolet-visible (UV-Vis) spectrophotometer (UV-6100, Metash, China), and the concentration of the nanoplastics in the aqueous phase was determined by measuring the UV absorbance at 220 nm (Supplementary Figure 9).

Exposure of *M. aeruginosa* to nanoplastics

M. aeruginosa (FACHB 905), purchased from the institute of hydrobiology, Chinese Academy of Sciences (Wuhan, China), was cultured in autoclaved standard blue-green (BG-11) medium at a pH of around 7.2. PS-NH_2 was added on the 10^{th} day of cyanobacterial growth. The systems without PS-NH_2, and those with PS-NH_2 at concentrations of 3.40 and 6.80 μg/mL were set as the control, low-concentration, and high-concentration exposure treatments, respectively. All the experiments were performed in six replicates. After acute (2 days) and long-term (10 days) exposure to PS-NH_2, the responses of *M. aeruginosa* by PS-NH_2 were investigated.

Analysis of microcystin, chlorophyll-a, and cell membrane integrity

M. aeruginosa samples were centrifuged at 10000 rpm and 4 °C for 5 min. The supernatant was used to analysis the extracellular microcystin. The residue was re-suspended in an original volume of ultra-pure water, and then frozen in liquid nitrogen and thawed at room temperature thrice. Then, the solution was centrifuged at 10000 rpm and 4 °C for 5 min. The supernatant was filtered through 0.22-μm acetate cellulose membranes for the analysis of intracellular microcystin. The extracellular and intracellular microcystin concentrations were detected using microcystin enzyme-

linked immunosorbent assay kits (Runyu Biotechnology CO., China). The chlorophyll-a analysis was performed based on the previous research.[27] The cell membrane integrity was evaluated according to the protocol[28,29]. The PS-NH_2 distribution in *M. aeruginosa* was observed through confocal microscopy. Confocal imaging was performed using a laser-scanning confocal microscope (LSM-700, ZEISS, Japan).

Analysis of antioxidant responses

M. aeruginosa samples were centrifuged at 10000 rpm and 4 °C for 5 min. The supernatant was discarded, and the residue was re-suspended in 300 μL of ultra-pure water. Then, the samples were frozen in liquid nitrogen and thawed at room temperature thrice. After centrifugation at 10000 rpm and 4 °C for 5 min, the supernatant was filtered through 0.22-μm acetate cellulose membranes for the analysis of the antioxidant responses of *M. aeruginosa.* Commercially SOD and GSH assay kits (Nanjing Jiancheng, China) were used to determine the activities of antioxidant enzymes, using a programmable microplate reader (Infinite F50, Tecan, Switzerland). The concentrations were normalized to the cell numbers before statistical analysis.

Analysis of Gene expression

Total RNA was extracted according to the procedures of Rnaprotect® Bacteria Reagent and Spin Column Bacteria Total RNA Purification Kit. The RNA concentration and purity were quantified by a nucleic acid analyzer. Before reverse transcription, a Primescript™ RT reagent kit with gDNA Eraser was utilized to remove genomic DNA contamination in RNA samples. The cDNA was then

synthesized through a process of reverse transcription polymerase chain reaction, which were stored at -20 °C until real-time qPCR analysis[30]. The primers of the 16S rRNA gene, which was used as the housekeeping gene, and *psbD* are shown in Supplementary Table 4[31].

Analysis of proteomic responses

M. aeruginosa cells were sampled in three biological replicates for the control and experimental groups during two phases: acute exposure (2 days) and long-term exposure (10 days). Protein extraction was performed via the trichloroacetic acid/acetone precipitation and the SDTLysis procedure[32]. After quantification, the proteins extracts were digested according to the filter-aided sample preparation (FASP) protocol procedure[33]. The iTRAQ labelled peptides were fractionated by strong cation exchange chromatography using the AKTA Purifier system. The collected fractions were desalted on C18 Cartridges and injected for nano-LC-MS/MS analysis. LC-MS/MS analysis was performed on a Q-Exactive mass spectrometer coupled to an Easy nLC. Protein identification was performed using the MASCOT engine embedded into Proteome Discoverer 1.4. To reduce the probability of false peptide and protein identification, the cutoff global false discovery rate was set to 0.01. Differentially expressed proteins were defined based on fold changes of > 1.2 or < 0.83 and a p value of < 0.05 in all three replicates. WGCNA was performed according to the R package of the WGCNA[34]. The PPI information of differentially expressed proteins was retrieved from the IntAct molecular interaction database using the STRING software, and the results were visualized via Cytoscape5 software (version 3.2.1). Furthermore, the degree of each protein was calculated to evaluate the importance of the protein in the PPI network**.**

Statistical analysis

All the experiments were run at least six independent experiments unless stated otherwise. For cell density evaluation, microcystin assay, gene expression, and antioxidant responses, one-way analysis of variance (ANOVA) with an unpaired *t* test were performed using Graphpad Prism. The differences were considered significant at $p < 0.05$ and, are referred to as $*p < 0.05$, $**p < 0.01$.

Data availability

The mass spectrometry proteomics data have been deposited to the ProteomeXchange Consortium via the PRIDE partner repository with the dataset identifier PXD011664. All other data are available from the corresponding author on reasonable request.

References

1. Wilcox C, Van Sebille E, Hardesty BD. Threat of plastic pollution to seabirds is global, pervasive, and increasing. *Proceedings of the National Academy of Sciences* **112**, 11899-11904 (2015).
2. Galloway TS, Lewis CN. Marine microplastics spell big problems for future generations. *Proceedings of the National Academy of Sciences* **113**, 2331-2333 (2016).
3. Nizzetto L, Langaas S, Futter M. Do microplastics spill on to farm soils? *Nature* **537**, 488 (2016).
4. Bornscheuer UT. Feeding on plastic. *Science* **351**, 1154-1155 (2016).
5. Rochman CM. Microplastics research—from sink to source. *Science* **360**, 28-29 (2018).
6. Lu Y, Mei Y, Walker R, Ballauff M, Drechsler M. 'Nano-tree' - type spherical polymer brush particles as templates for metallic nanoparticles. *Polymer* **47**, 4985-4995 (2006).
7. Dekkers S*, et al.* Presence and risks of nanosilica in food products. *Nanotoxicology* **5**, 393-405 (2011).
8. Pace ML*, et al.* Reversal of a cyanobacterial bloom in response to early warnings. *Proceedings of the National Academy of Sciences* **114**, 352-357 (2017).
9. Paerl HW, Otten TG. Blooms bite the hand that feeds them. *Science* **342**, 433-

434 (2013).

10. Michalak AM*, et al.* Record-setting algal bloom in Lake Erie caused by agricultural and meteorological trends consistent with expected future conditions. *Proceedings of the National Academy of Sciences*, 201216006 (2013).

11. Carmichael WW*, et al.* Human fatalities from cyanobacteria: chemical and biological evidence for cyanotoxins. *Environmental health perspectives* **109**, 663 (2001).

12. Jochimsen EM*, et al.* Liver failure and death after exposure to microcystins at a hemodialysis center in Brazil. *New England Journal of Medicine* **338**, 873-878 (1998).

13. Della Torre C*, et al.* Accumulation and embryotoxicity of polystyrene nanoparticles at early stage of development of sea urchin embryos Paracentrotus lividus. *Environmental science & technology* **48**, 12302-12311 (2014).

14. Okada U, Yamashita E, Neuberger A, Morimoto M, van Veen HW, Murakami S. Crystal structure of tripartite-type ABC transporter MacB from Acinetobacter baumannii. *Nature Communications* **8**, 1336 (2017).

15. Latifi A, Ruiz M, Zhang CC. Oxidative stress in cyanobacteria. *FEMS microbiology reviews* **33**, 258-278 (2009).

16. Zhang C, Yi Y-L, Hao K, Liu G-L, Wang G-X. Algicidal activity of Salvia miltiorrhiza Bung on Microcystis aeruginosa—Towards identification of algicidal substance and determination of inhibition mechanism. *Chemosphere* **93**, 997-1004 (2013).

17. Pearson LA, Hisbergues M, Börner T, Dittmann E, Neilan BA. Inactivation of

an ABC transporter gene, mcyH, results in loss of microcystin production in the cyanobacterium Microcystis aeruginosa PCC 7806. *Applied and environmental microbiology* **70**, 6370-6378 (2004).

18. Yeung AC*, et al.* Physiological and Proteomic Responses of Continuous Cultures of Microcystis aeruginosa PCC 7806 to Changes in Iron Bioavailability and Growth Rate. *Applied and environmental microbiology* **82**, 5918-5929 (2016).

19. Carman GM, Kersting MC. Phospholipid synthesis in yeast: regulation by phosphorylation. *Biochemistry and cell biology* **82**, 62-70 (2004).

20. Pimentel JS, Giani A. Microcystin production and regulation under nutrient stress conditions in toxic Microcystis strains. *Applied and environmental microbiology*, AEM. 01009-01014 (2014).

21. Liu Y, Chen S, Zhang J, Gao B. Growth, microcystin-production and proteomic responses of Microcystis aeruginosa under long-term exposure to amoxicillin. *Water research* **93**, 141-152 (2016).

22. Berenice E. Exposure to the herbicide 2, 4-D produces different toxic effects in two different phytoplankters: A green microalga (Ankistrodesmus falcatus) and a toxigenic cyanobacterium (Microcystis aeruginosa). *Science of the total environment*, (2017).

23. Moore CJ, Lattin G, Zellers A. Working our way upstream: a snapshot of land based contributions of plastic and other trash to coastal waters and beaches of Southern California. In: *Proceedings of the Plastic Debris Rivers to Sea Conference, Algalita Marine Research Foundation, Long Beach, CA* (ed^(eds) (2005).

24. Feng L-J, Wang J-J, Liu S-C, Sun X-D, Yuan X-Z, Wang S-G. Role of

376 extracellular polymeric substances in the acute inhibition of activated sludge
377 by polystyrene nanoparticles. *Environmental Pollution* **238**, 859-865 (2018).
378 25. Besseling E, Wang B, Lürling M, Koelmans AA. Nanoplastic affects growth
379 of S. obliquus and reproduction of D. magna. *Environmental science &*
380 *technology* **48**, 12336-12343 (2014).
381 26. Pikuda O, Xu EG, Berk D, Tufenkji N. Toxicity Assessments of Micro-and
382 Nanoplastics Can Be Confounded by Preservatives in Commercial
383 Formulations. *Environmental Science & Technology Letters*, (2018).
384 27. Zhu X, Kong H, Gao Y, Wu M, Kong F. Low concentrations of polycyclic
385 aromatic hydrocarbons promote the growth of Microcystis aeruginosa. *Journal*
386 *of hazardous materials* **237**, 371-375 (2012).
387 28. Huo X, Chang DW, Tseng JH, Burch MD, Lin TF. Exposure of Microcystis
388 aeruginosa to Hydrogen Peroxide under Light: Kinetic Modeling of Cell
389 Rupture and Simultaneous Microcystin Degradation. *Environmental science &*
390 *technology* **49**, 5502-5510 (2015).
391 29. Rasmussen RE, Erstad SM, Ramos-Martinez EM, Fimognari L, Porcellinis
392 AJ, Sakuragi Y. An easy and efficient permeabilization protocol for in vivo
393 enzyme activity assays in cyanobacteria. *Microbial cell factories* **15**, 186
394 (2016).
395 30. Guo N*, et al.* Effect of bio-electrochemical system on the fate and proliferation
396 of chloramphenicol resistance genes during the treatment of chloramphenicol
397 wastewater. *Water research* **117**, 95-101 (2017).
398 31. Qian H, Yu S, Sun Z, Xie X, Liu W, Fu Z. Effects of copper sulfate, hydrogen
399 peroxide and N-phenyl-2-naphthylamine on oxidative stress and the
400 expression of genes involved photosynthesis and microcystin disposition in

Microcystis aeruginosa. *Aquatic Toxicology* **99**, 405-412 (2010).

32. Wu L*, et al.* Comparative proteomic analysis of the maize responses to early leaf senescence induced by preventing pollination. *Journal of proteomics* **177**, 75-87 (2018).

33. Wiśniewski JR, Zougman A, Nagaraj N, Mann M. Universal sample preparation method for proteome analysis. *Nature methods* **6**, 359 (2009).

34. Voineagu I*, et al.* Transcriptomic analysis of autistic brain reveals convergent molecular pathology. *Nature* **474**, 380 (2011).

Acknowledgments

This work was supported by the National Science Foundation of China (No. 51478453, No. 21776163), the Qilu Youth Talent Programme of Shandong University and the Fundamental Research Funds of Shandong University (No. 2017JC021).

Authors information

Affiliations

Shandong Key Laboratory of Water Pollution Control and Resource Reuse, School of Environmental Science and Engineering, Shandong University, Qingdao, Shandong Province 266237, P. R. China

Li-Juan Feng, Jia-Qi Liu, Lin-Lin Zhou, Fan-Ping Zhu, Xiao-Dong Sun, Xiao-Yu Liu, Shu-Guang Wang, Xian-Zheng Yuan

College of Life and Environmental Sciences, University of Exeter, Exeter EX4 4QD, Devon, United Kingdom

Tamara S. Galloway

Contributions

X-Z. Yuan and L-J. Feng designed the experiments. X-Z. Yuan, L-J. Feng, T-S.

Galloway, and S-G. Wang wrote the manuscript. L-J. Feng, J-Q. Liu, L-L. Zhou, and X-Y. Liu performed the experiments. X-Z. Yuan, L-J. Feng, X-D. Sun, F-P. Zhu, and T-S. Galloway analyzed the results.

Competing interests

The authors declare no competing interests.

FIGURES

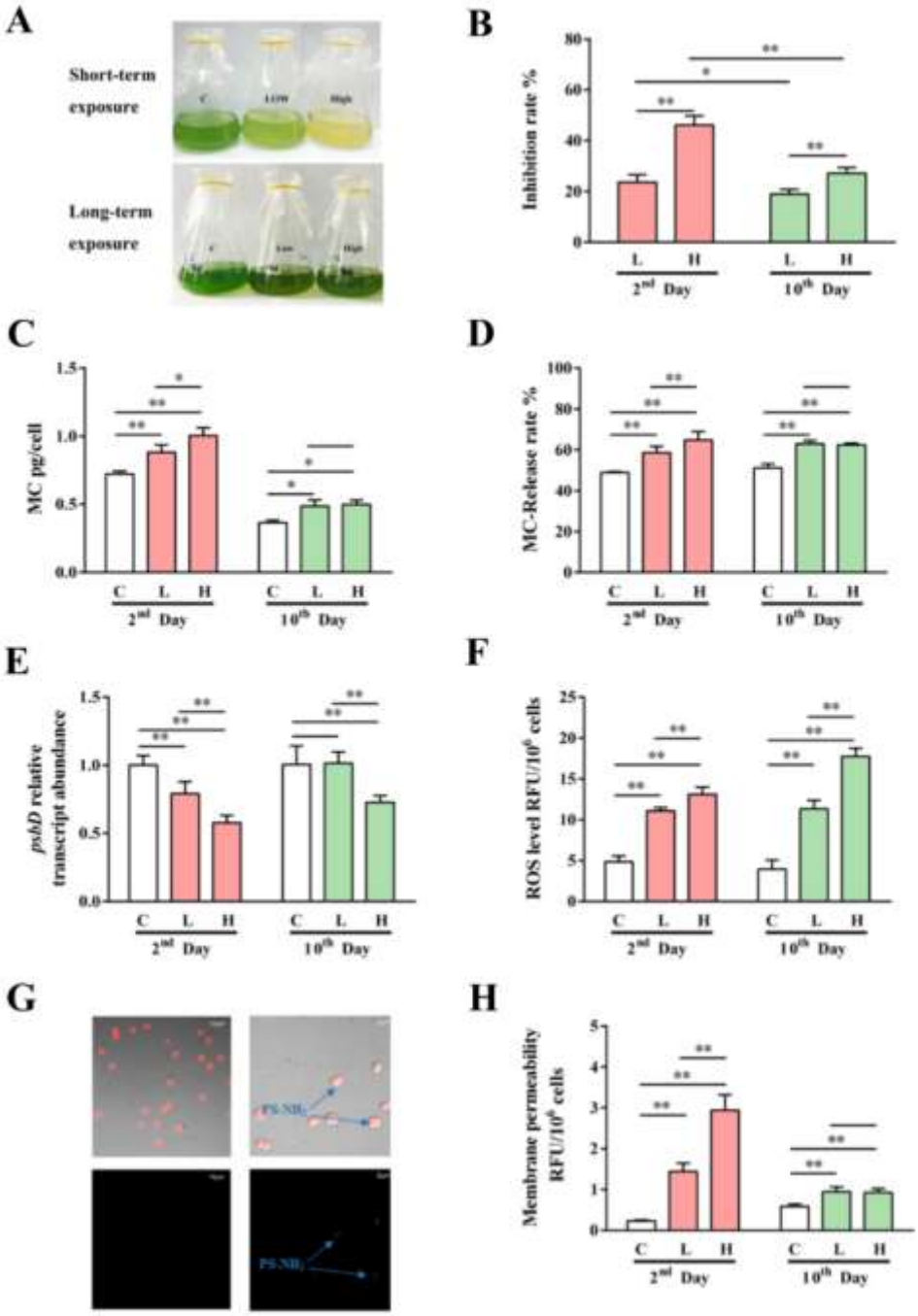

458

459 **Fig. 1 The response of *Microcystis aeruginosa* to acute and long-term exposure of**
460 **PS-NH_2.** Effects of PS-NH_2 after different exposure times on phenotype change (A),
461 growth inhibition rate (B), synthesis of total microcystin (C), release rate of
462 microcystin (D), transcriptional level of photosynthesis genes (E), ROS concentration
463 (F), location of PS-NH_2 in the cells (G) and cell membrane permeability (H). The
464 statistical significance was estimated by the two-tailed t-test and differences were
465 considered significant at $p < 0.05$, and are referred to as *$p < 0.05$, **$p < 0.01$.

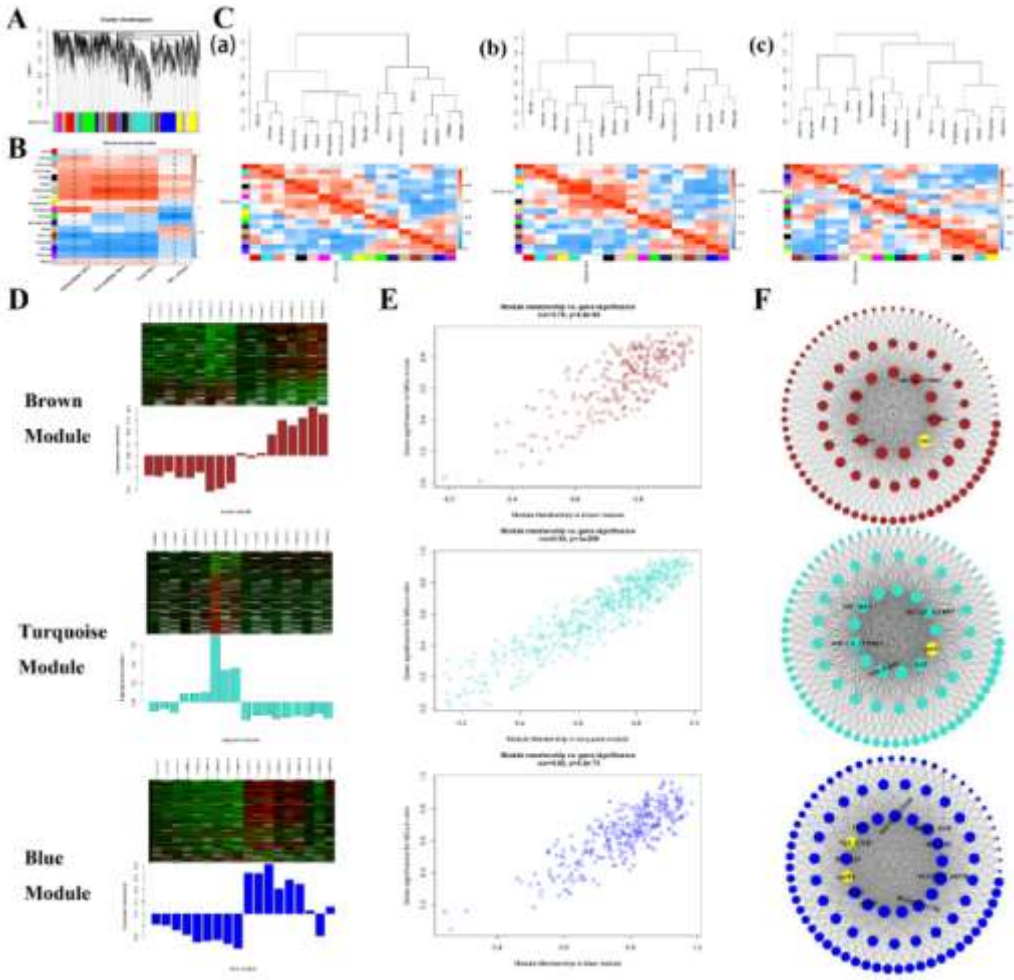

Fig. 2 The top hub proteins identified by WGCNA. (A) Clustering dendrograms of proteins, with dissimilarity based on topological overlap, together with assigned module colors. (B) Identification of protein modules associated with microcystin phenotypic traits. Each row corresponds to a module eigengene, while each column corresponds to a trait. Each cell contains the corresponding correlation and p value. The table is color-coded by correlation according to the color legend. (C) The eigengene dendrogram and heatmap identify groups of correlated eigengenes. The dendrogram (C, a) indicates that the magenta modules are highly related to intracellular microcystin. The dendrogram (C, b) indicates that the turquoise modules are highly related to extracellular microcystin. The dendrogram (C, c) indicates that no modules are highly related to microcystin release. (D) Heatmap of proteins in the module and eigengene expression in 18 samples. (E) A scatterplot of Gene Significance for different traits vs. Module Membership in the brown, turquoise, and blue modules. (F) The visualization of modules in the brown, turquoise, and blue module. The top hub proteins in the modules have been indicated in bold with a

yellow color.